Carbohydrate Polymers 101 (2014) 718–726

Contents lists available at ScienceDirect

Carbohydrate Polymers

journal homepage: www.elsevier.com/locate/carbpol

Effect of silanization on chitosan porous scaffolds for peripheral nerve regeneration

Guicai Li[a], Luzhong Zhang[a], Caiping Wang[a], Xueying Zhao[a], Changlai Zhu[a], Yanhong Zheng[a], Yaling Wang[b], Yahong Zhao[a], Yumin Yang[a,*]

[a] Jiangsu Key Laboratory of Neuroregeneration, Nantong University, Nantong 226001, PR China
[b] College of Chemistry and Chemical Engineering, Nantong University, Nantong 226001, PR China

ARTICLE INFO

Article history:
Received 19 August 2013
Received in revised form
16 September 2013
Accepted 18 September 2013
Available online 30 September 2013

Keywords:
Chitosan porous scaffolds
Silanization
Peripheral nerve regeneration
Schwann cells

ABSTRACT

The aim of this study was to evaluate the feasibility of using 3-aminopropyltriethoxysilane (APTE) silanization treatment for modification and biocompatibility of lyophilized chitosan porous scaffolds. The process is beneficial for biomaterial development due to its low toxicity and simplicity. The silanization treatment with low APTE concentration showed no significant influence on the morphology of chitosan scaffolds, while a skin-like surface was observed for the silanized scaffolds treated with high APTE concentration. The porosity and surface amino densities were increased after silanization whereas the swelling ratio was reduced, and the degradation ratio in PBS and anti-acid degradation properties of the silanized chitosan scaffolds were significantly improved. The *in vitro* Schwann cells culture demonstrated that the silanized scaffolds with 8% APTE could obviously facilitate the attachment and proliferation of Schwann cells, indicating great potential for the application in peripheral nerve regeneration.

1. Introduction

The peripheral nerve injury (PNI) is a serious health problem for the trauma patients caused by disease, war or traffic accident. Generally, an end-to-end anastomosis method can be used to bridge the PNI with small gaps, however, it is still difficult to completely cure the long nerve gaps (Ichihara et al., 2009). The autologous nerve graft is the best choice for repairing nerve injuries, but its source is limited and the wound at the donor site is permanent.

In recent years, a variety of biomaterials for better recovery of nerve functions have been developed (Hsu, Chan, Chiang, Chen, & Jiang, 2011; Kuo & Chang, 2013; Pettersson et al., 2011; Runge et al., 2010; Xu, Yan, & Li, 2011), including natural and synthetic polymers. Chitosan (CS), as a natural polysaccharide, has attracted more and more attention due to its good biocompatibility, biodegradability, non-toxicity, readily availability and unique physicochemical properties (Busilacchi, Gigante, Mattioli-Belmonte, Manzotti, & Muzzarelli, 2013; Qu, Lin, Zhang, Xue, & Zhang, 2013; Wang et al., 2005; Wlaszczuk, Pietrucha-Dutczak, Marcol, Jedrzejowska-Szypulka, & Lewin-Kowalik, 2011; Yang et al., 2011; Yuan, Zhang, Yang, Wang, & Gu, 2004), and have been used in various areas of tissue engineering (Muzzarelli, 2009). Yuan et al. studied the interaction of Schwann cells with chitosan scaffolds and fibers, and found that both the chitosan scaffolds and fibers had excellent neuroglial cell affinity, suggesting a promising application of chitosan for nerve regeneration (Yuan et al., 2004). Wei et al. fabricated the collagen–chitosan scaffold and further immobilized RGD sequences to mimic the bio-functional peripheral nerve, they found that this scaffold could promote rapid regeneration of injured sciatic nerve in rats (Xiao et al., 2013). The chitosan/gelatin nerve graft was also developed for delivering Schwann cells and nerve growth factor (NGF) to explore the feasibility of improving sciatic nerve regeneration, the results showed that the nerve conduction velocity, average regenerated myelin area, and myelinated axon count were all promoted (Nie et al., 2013). Xu et al. developed a more complex conduit composed of poly-DL-lactide, chondroitin sulfate and chitosan, and further immobilized NGF on the conduit with carbodiimide, the conduit was found to enhance rapid functional recovery of the disrupted nerve without connective tissues from ingrowth, indicating the conduit would be useful material to repair peripheral nerve damage (Xu et al., 2011). In addition, the differentiation of induced pluripotent stem (iPS) cells into neuron-like cells was found to be accelerated by the chitin–chitosan–gelatin scaffolds (Kuo & Lin, 2013). As mentioned above, despite the wide range of chitosan related biomaterials for nerve repair available, it is still unacceptable about the functional recovery of seriously injured nerve due to the scar formation, which may inhibit the regeneration process. Therefore, it is necessary to further improve the properties of chitosan for promoting nerve regeneration *via* various physicochemical methods.

* Corresponding author. Tel.: +86 0513 8505 1818; fax: +86 0513 8551 1585.
E-mail address: yangym@ntu.edu.cn (Y. Yang).

0144-8617/$ – see front matter © 2013 Elsevier Ltd. All rights reserved.
http://dx.doi.org/10.1016/j.carbpol.2013.09.064

Generally, the biomaterials surface plays an important role on cell response to the implants, thus surface modification of the biomaterials will be beneficial for improving the biocompatibility. Silanization is a convenient method that can be used to cover the biomaterials surface through the covalent binding of organofunctional alkoxysilane molecules and surface hydroxyl groups. Aminosilanes display potentially useful because they could be used to directly or indirectly (through a linker) immobilize biomolecules on biomaterials surface (Baggi, Boschi, Caleffi, Martignoni, & Venanzi, 1990), which are important for subsequential cell or tissue responses. Various silane agents have been applied to modify the inorganic and organic biomaterials surface in terms of different purposes, including glass (Halliwell & Cass, 2001), dental ceramics (Matinlinna & Vallittu, 2007), titanium (Li et al., 2011) and natural fiber/polymer composites (Salon, Abdelmouleh, Boufi, Belgacem, & Gandini, 2005). 3-Aminopropyltriethoxysilane (APTE) is one of the most widely used silane agents for fabricating the amine-terminated scaffolds (Kim, 2011; Lapin & Chabal, 2009). Yoshioka, Tsuru, Hayakawa, and Osaka (2003) reported that the alginic acid layers immobilized on gamma-APTE-grafted stainless-steel could obviously inhibit platelet adhesion and improve blood compatibility. Li et al. (2011) grafted heparin/fibronectin complex on titanium surface *via* APTE silanization, and showed that the modified surface could simultaneously promote endothelialization and inhibit thrombosis formation. In most cases, APTE is used to silanize inorganic biomaterials surface in order to provide amino reactive sites for biomolecules grafting. Though there are some reports referring to the silanization of different polymers (Gan, Yang, & Yang, 2009; Salon et al., 2005), the effect of silanization treatment on the natural biomaterials is still unknown, especially for the biological response.

In the present study, the feasibility of using APTE to silanize the lyophilized chitosan scaffolds was evaluated. The effects of silanization on the scaffolds performances including morphology, porosity, swelling rate and degradation behavior were measured. The primary Schwann cells were seeded on the sterilized scaffolds and cultured statically *in vitro* for different periods. The attachment and proliferation behaviors of the cells on silanized chitosan scaffolds were investigated.

2. Materials and methods

2.1. Materials

Chitosan powder (Mw: 2.8×10^4) with a degree of deacetylation of 92.3% was purchased from Nantong Xincheng Biochemical Company, Jiangsu, China. 0.067 M phosphate buffer saline (PBS, pH 7) and Dulbecco's modified eagle medium (DMEM) were purchased from Hyclone Co., Ltd. Forskolin, heregulin, 3-aminopropyltriethoxysilane (APTE), Toluidine blue O (TBO) and acid orange II (AO II) were all purchased from Sigma–Aldrich. A 1 wt% acetic acid solution was prepared by diluting 1 mL acetic acid in 100 mL deionized water (dH_2O). All the other reagents used in the experiments were of the highest analytical purity (>99.9%).

2.2. Preparation of the silanized chitosan scaffolds

The preparation of the silanized chitosan scaffolds is systematically shown in Fig. 1. Firstly, the chitosan scaffolds were prepared using the following method: the chitosan powder was dissolved in a 1 wt% acetic acid aqueous solution to form a 1 wt% chitosan solution at room temperature, the solution was stationary for 2 h to remove the trapped air bubbles. Subsequently, the chitosan solution was poured into a cell culture dish and lyophilized in a freeze dryer at −50 °C for 24 h to form porous chitosan scaffolds. After the drying stage, the formed chitosan scaffolds were immersed in a 0.1 M NaOH aqueous solution for 24 h to neutralize the residual acetic acid. Then the scaffolds were rinsed with dH_2O for 8∼10 times to remove the residual alkali. Finally, the scaffolds were dried and stored in dehumidifying device before use. Secondly, the silanized chitosan scaffolds were prepared using silanization method as follows: the chitosan scaffolds above were silanized by immersing into a 2%, 5% and 8% v/v solution of the APTE in anhydrous ethanol for 5 h, respectively. The silanized chitosan scaffolds by APTE was separately denoted CSA-2%, CSA-5% and CSA-8%, then the samples were washed thoroughly with ethanol in order to remove the physisorbed APTE molecules. After that, the samples were kept in a 120 °C oven for 6 h to enhance the binding of APTES with the chitosan scaffolds.

2.3. Morphology of the prepared chitosan scaffolds

The surface morphology of the prepared chitosan scaffolds was observed using an optical microscopy (OM, Leica, Germany) and a scanning electron microscopy (SEM, Hitachi S-3400 NII, Japan), respectively. For SEM observation, briefly, the test samples were fixed to an aluminum stage using a double-sided adhesive tape, and then coated with gold to a thickness of 50 nm using a gold sputter coater machine. Finally, the coated samples were observed by SEM under the vacuum degree of 1.33×10^{-4} Pa.

2.4. FTIR

The infrared absorption spectra of the pristine chitosan, CSA-2%, CSA-5%, and CSA-8% were obtained from a FTIR spectrometer (Nicolet5700, Madison, WI) in transmission mode. For each spectrum obtained, a total of 64 scans were accumulated at 4 cm^{-1} resolution. Scanning was conducted in the range from 400 to 4500 cm^{-1}.

2.5. Porosity rate

The porosity rate of the chitosan scaffolds before and after silanization was measured by a liquid displacement method reported by Yoshioka et al. (2003). Briefly, the scaffold was immersed in anhydrous ethanol with a known volume (V_0), and then a series of vacuum-release cycles were performed to force the liquid into the pores of the scaffold. Thereafter, the volume of the liquid-perfused scaffold and liquid was recorded as V_1. Subsequently, the liquid-perfused scaffold was taken out, and the remaining liquid volume was recorded as V_2. Finally, the porosity rate of the scaffolds was calculated using the following equation:

$$\frac{V_0 - V_2}{V_1 - V_2} \times 100\%$$

2.6. Measurement of amino groups

The density of the amino groups was determined by AO experiment as following: the chitosan samples were immersed in 500 μmol/L AO-hydrochloric acid (HCl) (pH 3) solution dissolved in water. After shaking for at least 1 h at 37 °C, the samples were rinsed three times with pH 3 HCl solution. Then, the samples were immersed into pH 12 NaOH solution and shaken for 15 min at room temperature to dissolve the adsorbed AO. Finally, 150 μL of desorbed AO supernatant was added to a 96-well plate, and the optical density (OD) was recorded with a microplate reader (Bio-Tek Inc.,

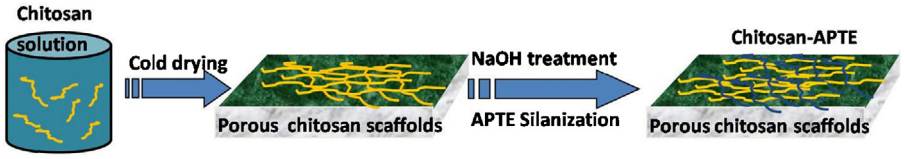

Fig. 1. Illustration of the preparation of silanized chitosan scaffolds.

USA) at 485 nm. The AO concentration was parallel to the density of amino groups on the samples.

2.7. Swelling ratio

The swelling ratio of the chitosan scaffolds before and after silanization was investigated by immersing the scaffold in a phosphate-buffered saline (PBS, pH 7) at 37 °C for 24 h. Thereafter, the chitosan scaffold was taken out and dried by sandwiching the scaffold between two paper towels in order to remove the excess water on the surface, and then the scaffold was weighted immediately. The swelling ratio of the chitosan scaffold in PBS was calculated using the following expression:

$$R_{sw} = \frac{W_s - W_d}{W_d} \times 100\,\%$$

where W_d is the weight of the dried chitosan scaffold, and W_s is the weight of the swollen chitosan scaffold.

2.8. In vitro degradation test

The *in vitro* degradability of chitosan scaffolds after silanization was performed using PBS and HCl, respectively. The samples were separately immersed in PBS (pH 7) or HCl (pH 3) at 37 °C and shaken (100 rpm) for different times (for HCl: 1, 3, 5 and 7 h; for PBS: 1, 3, 7, 14 and 28 d) in a sealed container, and the samples without silanization were used as reference. Then all the soaked samples and reference samples at each time point were taken out and dried, and the weight of the samples were measured by electronic balance. In addition, the morphology of the samples after immersion in HCl for certain time was photographed. Finally, the *in vitro* degradation rate was calculated as:

$$\frac{W_b - W_a}{W_b} \times 100\%$$

where W_b is the weight of the dried chitosan scaffold before degradation, and W_a is the weight of the dried chitosan scaffold after degradation.

2.9. Schwann cell culture

Schwann cells were harvested and cultured on samples using the following method: The sciatic nerves were excised from 2 to 5 day old Sprague–Dawley rat pups and enzymatically digested with 1% collagenase and 0.125% trypsin at 37 °C for 40 min. Then, the mixture was centrifuged and resuspended in DMEM with 10% fetal bovine serum (FBS), and the cell suspension was added in the petri dishes. After incubation for 24 h, the Schwann cells were purified by adding 10 mM cytosine arabinoside to the above dishes and incubated for additional 48 h to remove fibroblasts. Subsequently, 2 mM forskolin and 2 ng/mL heregulin were used to stimulate cell proliferation. Thereafter, the cells were incubated at 37 °C for 7 days in a humid 5% CO_2 atmosphere before use.

After a 7-day incubation, the primary Schwann cells were digested and cultured on samples. The chitosan scaffolds with or without silanization were sterilized in a steam autoclave at 120 °C for 2 h, subsequently, all the sterilized samples were placed in a 24-well culture plate and 1 mL cell suspension was added in. The concentration of Schwann cells for seeding on the samples was 1×10^5 cells/mL. Finally, the morphology and quantity evaluation were performed after the samples incubation for 1 d, 3 d and 5 d, respectively.

2.10. Cell morphology observation

The morphology of Schwann cells on different samples was examined by TBO staining method. Briefly, the samples were rinsed thoroughly with PBS for three times to remove non-adhering cells and fixed with 4% (w/v) paraformaldehyde for 30 min. Then, the samples were rinsed with PBS and blocked with 1% BSA at 37 °C for 30 min to block nonspecific binding and rinsed with PBS for three times. Subsequently, TBO dye solution was prepared as follows: 1 g TBO was firstly diluted in 100 mL 70% alcohol and thus 1 wt% TBO-alcohol solution was obtained, then the TBO work solution (1 mg/mL) was prepared by further diluting 1 wt% TBO-alcohol solution in 0.9 wt% sodium chloride. Thereafter 1 mL TBO work solution was added on the samples and incubated for 30 min at room temperature and rinsed with PBS for three times. Finally, the stained samples were observed under an optical microscope (Leica, Germany).

2.11. Cell quantity analysis by cck-8 kit

CCK-8 kit was used to evaluate the amount of cells on different samples after culture for 1, 3 and 5 days, respectively. All the sterilized samples were placed in a 24-well culture plate and 1 mL Schwann cells suspension with 1×10^5 cells/mL was added. After 4 h, the medium was removed and non-adherent cells were rinsed off with PBS for twice. Subsequently, fresh medium (without phenol red) containing CCK-8 reagent (10× diluted in medium) was added to each sample and incubated at 37 °C for 4 h in standard culture conditions. Afterwards, 200 μL/well of the suspension was transferred to a 96-well plate. The absorbency was measured at 450 nm by a microplate reader.

2.12. Data analysis

The data were analyzed with the software SPSS 11.5 (Chicago, Illinois). Statistical evaluation of the data was performed using one-way ANOVA method. The probability (P) values $P < 0.05$ were considered to be statistically significant differences. The results were expressed as mean ± standard deviation (SD).

3. Results and discussion

3.1. Morphology of the prepared chitosan scaffolds

The morphology of the prepared chitosan scaffolds observed by optical microscope is shown in Fig. 2. It could be seen from the optical microscope results that there was no obvious morphological difference for all the chitosan scaffolds with or without silanization, and a lot of filamentous structure could be seen for all the samples. However, the SEM results showed that the microstructure of the scaffolds was different, though all the chitosan scaffolds displayed highly porous structure with thin walls and three-dimensional interconnected pores. As shown by SEM, the surface morphology

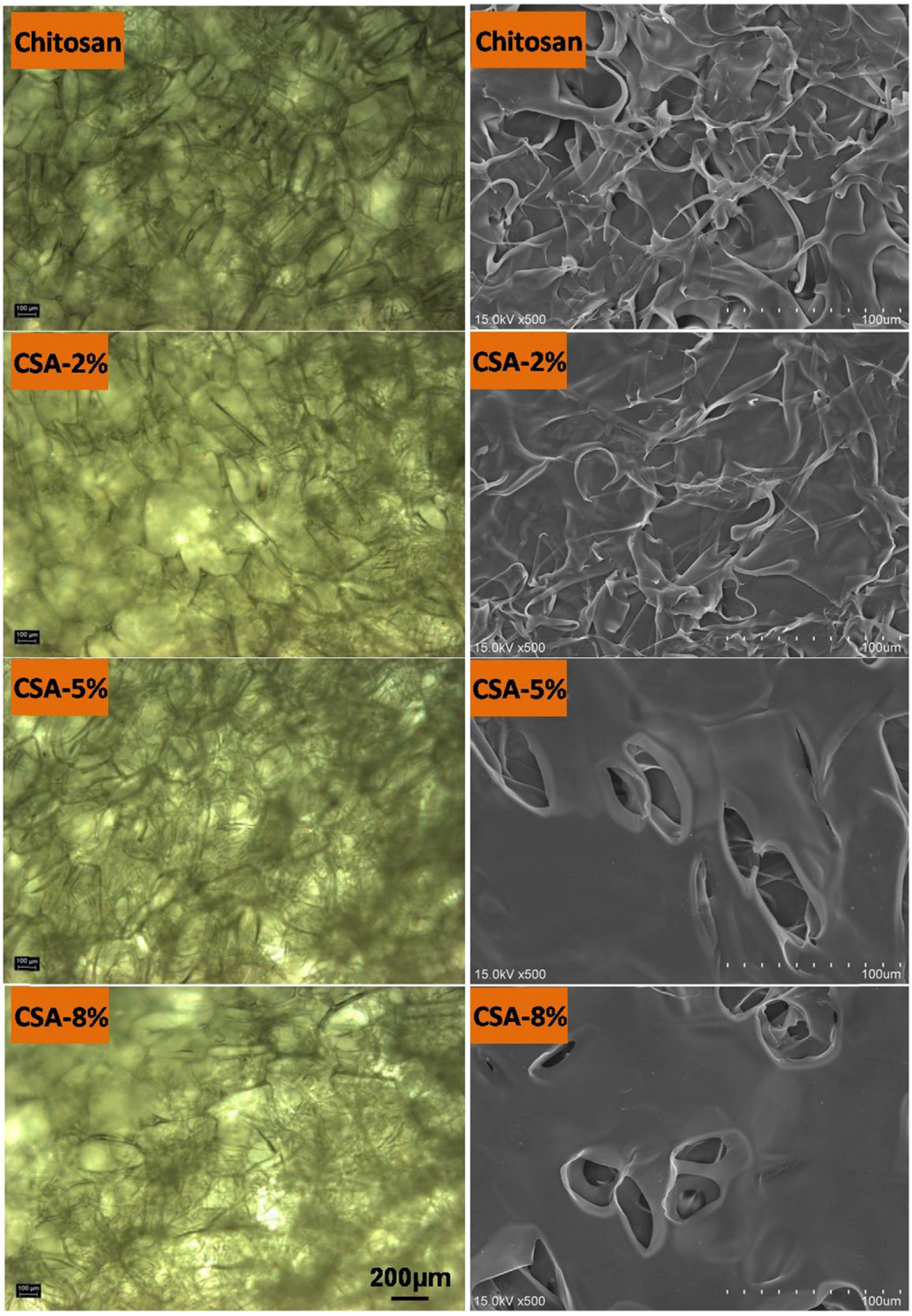

Fig. 2. Phase contrast microscopy (upper row) and SEM (lower row) images of the unsilanized and silanized chitosan scaffolds on a view from surface, respectively.

of chitosan and CSA-2% scaffolds was cluttered with plenty of fiber- and strip-like structure, the silanization with low APTE concentration did not cause obvious difference of the chitosan scaffolds surface. Whereas the surfaces of CSA-5% and CSA-8% scaffolds silanized with higher APTE concentration displayed a skin-like structure with many oval pores on them instead of a fiber-like structure, and the average size of pores (40–80 μm) was almost the same. The pores on scaffolds could supply oxygen and nutrients for the cells. It was reported that the pore size of scaffold regulated the angiogenes processes (Annabi et al., 2010). The optimal pore size usually depended on different cell types, an average pore diameter from 20 μm to 125 μm was shown optimal morphological active for skin regeneration (Yannas, Lee, Orgill, Skrabut, & Murphy, 1989), whereas osteoblasts displayed favorable attachment to pore in the size more than 100 μm (Byrne et al., 2008). The results indicated that the morphology of chitosan scaffolds could be changed by APTE silanization, which may be ascribed to the grafting of APTE molecules during silanization processing, but the exact reasons for variation in morphology were still under investigation.

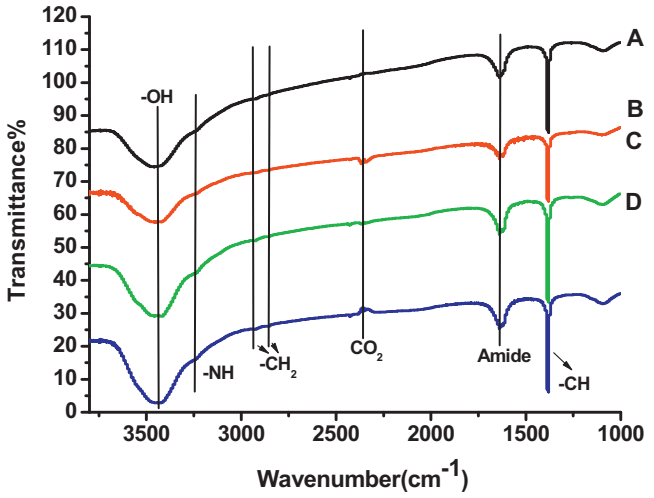

Fig. 3. FTIR spectroscopy of (A) chitosan, (B) CSA-2%, (C) CSA-5%, and (D) CSA-8%.

3.2. Fourier transform infrared spectroscopy (FTIR) analysis

The surface properties of the chitosan scaffolds before and after silanization were characterized by FTIR (Fig. 3). It could be seen that compared with the original chitosan scaffolds, CSA-2% sample showed almost no new peaks appearance except for the absorption in about 2400 cm^{-1}, which was corresponding to the CO_2 from the air, the differences were caused by the background remove, however, the determination of other special groups could not be affected by this peak. Then after silanized with high APTE concentration, *i.e.* CSA-5% and CSA-8%, the scaffolds showed larger —OH and —NH peaks in 3400 cm^{-1} and 3200 cm^{-1} than chitosan and CSA-2% samples, respectively. Moreover, the CSA-5% and CSA-8% samples showed new weak peaks in 2900 cm^{-1} corresponding to $-CH_2$ and —CH. The increased —OH peak was mainly due to the reaction between the —OH groups on chitosan and those on APTE, while the $-CH_2$ and $-CH_3$ groups were mainly from APTE molecules. In addition, both the peaks in 1620 cm^{-1} and 1400 cm^{-1} were corresponding to the C=O stretching vibrations for amide I, II and C—H bending vibrations, respectively. The FTIR results further demonstrated that the silanization treatment with lower concentration of APTE had weak effect on chitosan scaffolds, whereas APTE with higher concentration could cause the change of chitosan properties. The underlying mechanism might be anticipated that the chitosan properties were rather stable with long chain structure and thus APTE with lower concentration was not enough to react with all hydroxyl groups and change its properties, and the porous structure of chitosan scaffolds may also affect the silanization processing due to the trap of APTE in pores, thus the effect of silanization with low concentration of APTE was not obvious. Whereas APTE with high concentration was enough to react with chitosan and reduced the effect of chitosan scaffolds in *per se*. However, further work should be performed to verify that in our future study.

3.3. Porosity rate

Porosity plays an important role in the scaffolds used in peripheral nerve regeneration, because the pores can provide nutrition for cells and tissue. The porosity of different samples is shown in Fig. 4, it was found that the porosity of single chitosan scaffolds was about 81%, while significantly increased to about 88% after APTE silanization ($P < 0.05$), moreover, there was no statistical difference among the silanized samples ($P > 0.05$). Peng, Cheng, Wang, Xu, and Wang (2006) fabricated chitosan/collagen scaffolds for periodontal tissue engineering and found that the porosity

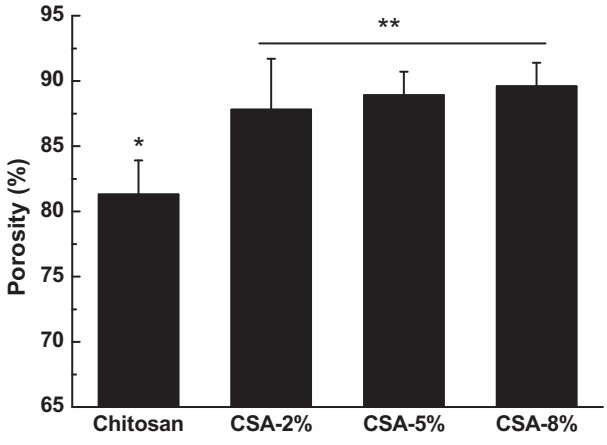

Fig. 4. Porosity of the scaffolds, $^{*}P < 0.05$ compared with APTE silanized samples; $^{**}P > 0.05$ among the silanized scaffolds.

of single chitosan scaffolds was more than 90%, which was significantly higher than that in our study. The difference may be caused by the experiment details, especially for the lyophilization steps. In the literature, several lyophilization steps were perfomed while in our study just one lyophilization step was conducted. Thus it was reasonable to believe that the porosity and pore size would be enlarged with more lyophilization steps. However, the surface morphology of CSA-2% was very different from those of CSA-5% and CSA-8% samples, the porosity showed no obvious difference for the three silanized samples. Generally, the suitable aperture, homogeneous microstructure and high porosity are the characteristics for the ideal porous scaffolds used in tissue engineering. The more space and nutrition for the cells and tissue will be provided by the higher porosity of scaffolds than the lower one. Thus based on the hypothesis above, the silanized chitosan scaffolds with higher porosity in our study will be better than the single chitosan scaffolds in tissue engineering application.

3.4. Amine concentration by the AO test

The amine concentrations on the scaffolds were quantitatively characterized using the AO test. The results are shown in Fig. 5, it could be seen that the amino concentration on unmodified chitosan scaffolds was about 59 nmol/cm^2, and there was no obvious difference after silanization with 2% APTE. However, after silanization with 5% and 8% APTE, there was a significant increase ($P < 0.05$)

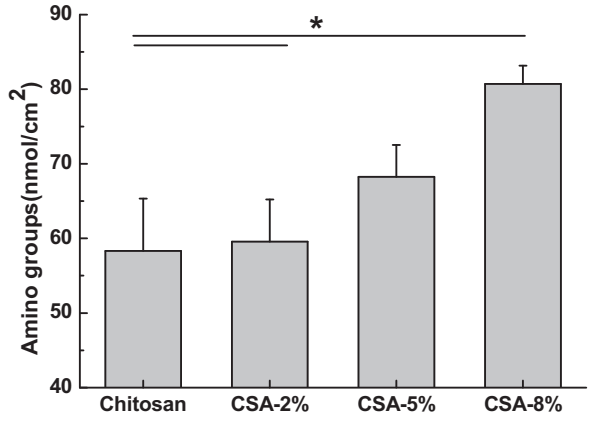

Fig. 5. Surface amine concentration of single chitosan scaffolds and silanized chitosan scaffolds ($^{*}p < 0.05$ compared with CSA-5% and CSA-8%).

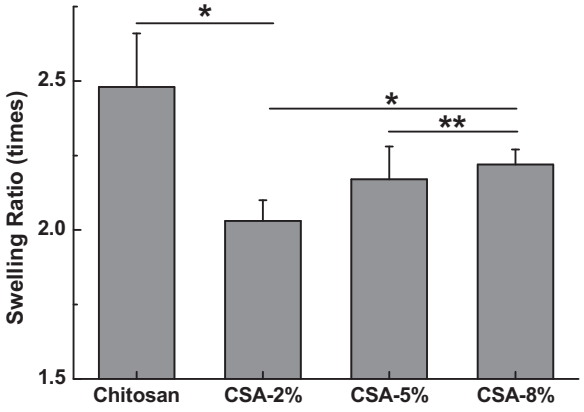

Fig. 6. The swelling behavior of single chitosan scaffolds and silanized chitosan scaffolds, $^{*}P < 0.05$, $^{*}P > 0.05$.

of amino concentration to 68 nmol/cm^2 and 80 nmol/cm^2, respectively. The results further indicated that the silanization treatment with 2% APTE could not cause slight variation of amino concentration and physicochemical properties of chitosan scaffolds, whereas the higher APTE concentration could induce larger amino concentration. The amino groups were reported to improve the cell proliferation ratios on amino-modified polycaprolactone by Zhu, Gao, Liu, and Shen (2002), thus the increase of amino concentration of silanized chitosan scaffolds was expected to improve cell attachment and proliferation.

3.5. Swelling ratio

The swelling property of scaffolds is very important for the nutrition and waste exchange *in vitro* and *in vivo*. Fig. 6 shows the swelling ratio of chitosan scaffolds and silanized chitosan scaffolds in PBS at 37 °C, after 24 h immersion the swelling ratio of single chitosan scaffolds was about 2.4 times, whereas significantly decreased to about 2 times after silanization with 2% APTE ($P < 0.05$). Then the swelling ratio further increased to 2.2 times after silanization with higher APTE concentration. It could be seen that the swelling ratio of all the silanized chitosan scaffolds were significantly lower than those of single chitosan scaffolds. The reason might be that APTE was a kind of coupling agent, which could react with the hydroxyl groups on chitosan scaffolds, moreover, the APTE molecules could also crosslink with each other (Howarter & Youngblood, 2006). In addition, the hydrophilicity and charged groups may influence the swelling property, the intermolecular crosslinking consumed hydroxyl groups and reduced the hydrophilicity (Hennink & van Nostrum, 2002), thus the silanization treatment reduced the swelling properties of the chitosan scaffolds. Notablely, there was significantly difference of the swelling ratio between CSA-2% and CSA-5% ($P < 0.05$), but no obvious difference was observed for CSA-5% and CSA-8% ($P > 0.05$), indicating that the swelling property almost reached a balance using high APTE concentration. The results were consistent well with the SEM observation.

3.6. In vitro degradation

The stability of the silanized chitosan scaffold was evaluated *via* the *in vitro* studies of the degradability in either a PBS solution and a HCl solution (pH 3) at 37 °C for different periods, respectively. The results are shown in Fig. 7, it could be seen that the degradation ratio of single chitosan scaffolds increased dramatically to about 7% after immersion in PBS for 1 d (Fig. 7A), and there was no obvious variation during the immersion periods from 1 d to 28 d.

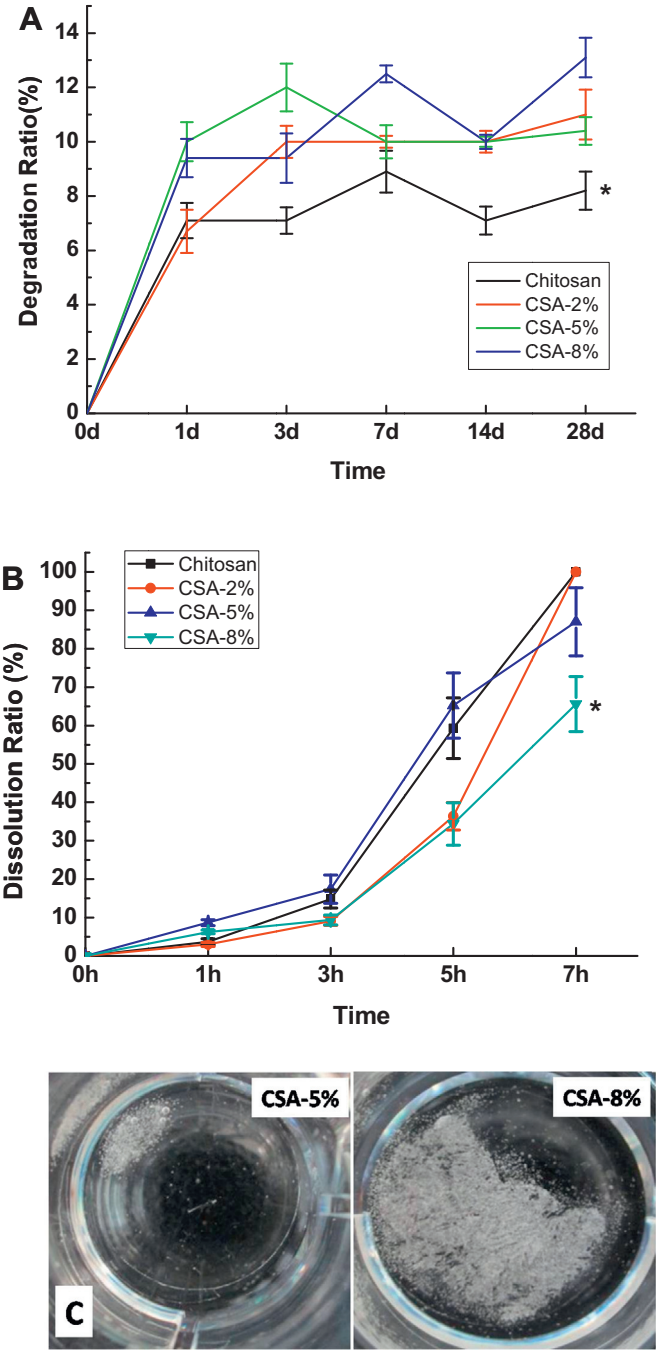

Fig. 7. Dry weight after *in vitro* stability of chitosan scaffolds before and after silanization as a function of time. (A) in PBS (B) in HCl and (C) photographs of CSA-5% and CSA-8% scaffolds after immersion in HCl for 7 h. $^{*}P < 0.05$ compared with other samples.

Compared with the single chitosan scaffolds, all the silanized scaffolds showed a significant increase of the degradation ratios from 9% to 13% ($P < 0.05$), while there was no obvious difference among the three silanized samples, the reason may be ascribed to the hydrolysis of APTE in PBS (Salon et al., 2005). In addition, the surface morphology of all the scaffolds displayed no change compared with the samples without PBS immersion (data not shown). The above results demonstrated that the chitosan scaffolds showed only little degradation during the periods, indicating the poor degradation property of chitosan, which was consistent well with the report by Zhang et al. (2013).

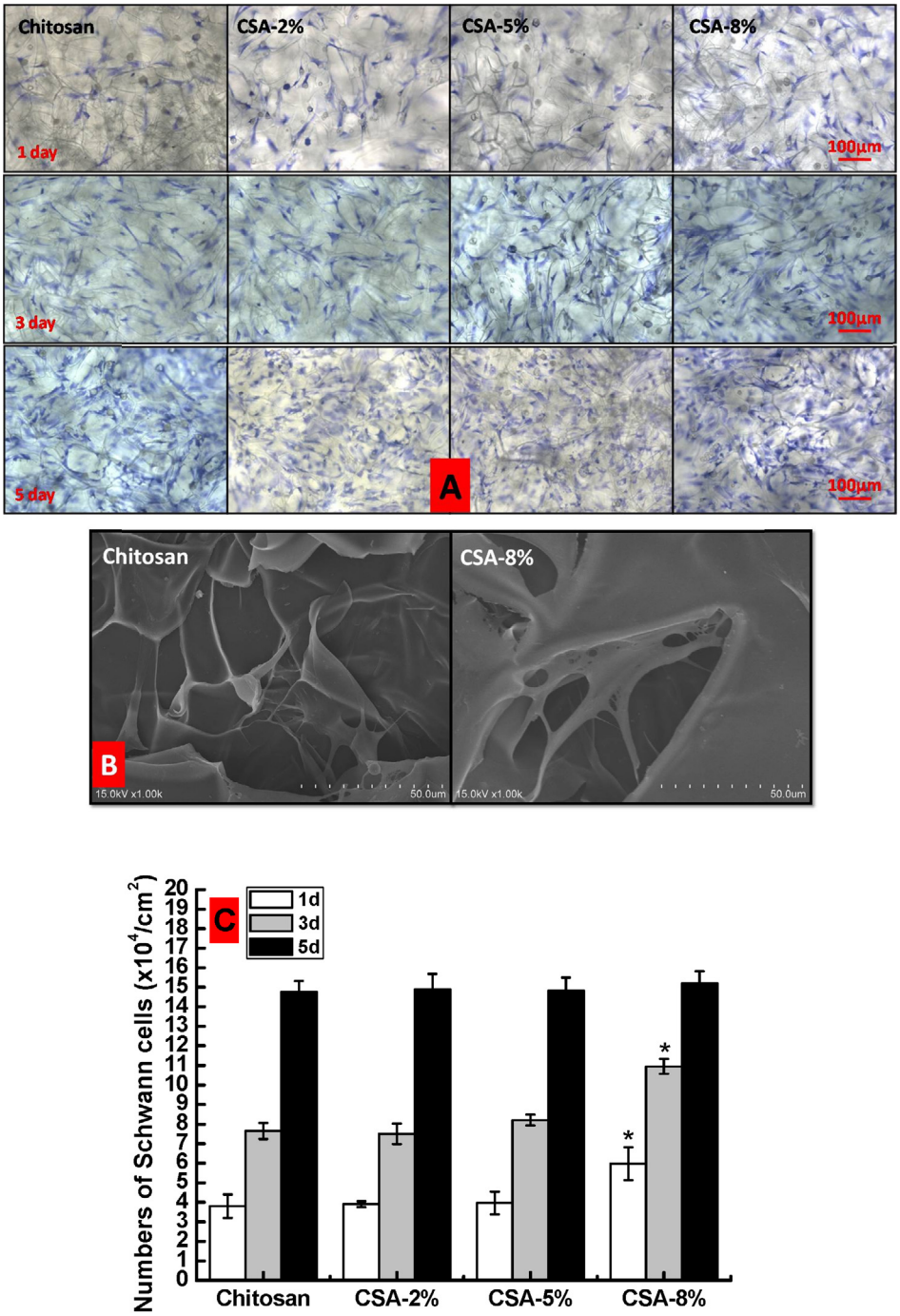

Fig. 8. *In vitro* Schwann cell culture on single chitosan scaffolds and silanized chitosan scaffolds for 1, 3 and 5 days, respectively. (A) Representative optical micrographs of Schwann cells, (B) representative SEM micrographs of Schwann cells after 5 d culture, and (C) number of Schwann cells on different scaffolds by CCK-8 test, $^{*}P < 0.05$, compared with other samples.

Fig. 7B shows the dissolve behavior of the chitosan scaffolds in HCl solution for a short time, the results showed that the dissolve ratios for all the scaffolds were less than 10% in the 1 h. However, the dissolve ratios significantly increased after 3 h incubation, the single chitosan and CSA-2% scaffolds had larger dissolution than CSA-5% and CSA-8% ($P < 0.05$). And after 7 h incubation, it could be seen that the single chitosan and CSA-2% scaffolds dissolved completely, and about 90% of the CSA-5% scaffolds dissolved, whereas the CSA-8% scaffolds only showed a dissolve ratio of about 65%, which was significantly lower than the other samples ($P < 0.05$). The above results was an important reference for the AO test due to the existance of HCl, because if the samples were incubated more than 1 h, then the serious dissolution of the scaffolds by HCl would occur, which may affect the real measurement results of amino groups, thus the incubation time with 1 h was selected. The morphology of the samples after immersion in HCl for 7 h was also observed (Fig. 7C), the chitosan scaffolds with 5% APTE concentration lost their integrity and were reduced to fragments, while the silanized scaffolds with 8% APTE showed retained much of their original shape. The results indicated that with the increased APTE concentration, the silanized chitosan scaffolds possessed higher anti-acid dissolve properties. The study of the stability of chitosan scaffolds above suggested silanization may improve their durability and half-life *in vivo*.

3.7. Evaluation by Schwann cells

Schwann cells are the most frequently used cells for evaluating the peripheral regeneration process (Chiono, Tonda-Turo, & Ciardelli, 2009), because they could produce growth factor and secrete extracellular matrix for the formation of myelin sheaths in nerve regeneration (Gu et al., 2012; Yuan et al., 2004). Thus, in this study Schwann cells culture were used to preliminary assess the feasibility of using the silanized chitosan scaffolds for further application in peripheral nerve regeneration. Fig. 8A and B shows the morphology and viability of Schwann cells cultured on various samples for 1, 3 and 5 d, respectively. The cell staining by TBO was observed using optical microscope (Fig. 8A) and showed that Schwann cells were able to attach on all scaffolds surface and could penetrate into the porous structure of the scaffolds after culture for 1 d. The cells mainly displayed long olivary shape on the samples at 1 d and 3 d, and there were no morphological changes in cells on the silanized chitosan scaffolds when compared with those on single chitosan scaffolds. Whereas the cells showed spherical shape at the 5 d on all the samples, indicating an almost confluent cell adlayer, the cell morphology here was consistent well with the study by Yuan et al. (2004). The SEM results were further used to observe the detailed skeleton distribution of Schwann cells on different samples, the typical SEM images of Schwann cells cultured for 5 days on single chitosan scaffolds and CSA-8% are shown in Fig. 8B. Only the image of CSA-8% was shown here because there was no skeleton difference of Schwann cells on CSA-8% compared with that on CSA-2% and CSA-5%. The cells on both single chitosan scaffolds and CSA-8% displayed the similar skeleton distribution with axons spreading out, and Schwann cells mainly attached in the pores of the silanized scaffolds.

CCK-8 test was further used to evaluate the viability of Schwann cells on chitosan scaffolds (Fig. 8C), it could be seen that there was no obvious difference of the cell amount for chitosan, CSA-2% and CSA-5% scaffolds during the whole incubation periods ($P < 0.05$). However, the number of Schwann cells was increased dramatically on CSA-8% scaffolds at 1 d and 3 d compared with those on other samples ($P < 0.05$), indicating better cell proliferation on the silanized scaffolds with high APTE concentration. But at the 5 d, no obvious difference of the Schwann cells number on all the samples was observed ($P > 0.05$). The results were also in accordance with the morphology observation of the cells in Fig. 8A. Despite no cell number difference at the 5 d, the *in vitro* cell culture demonstrated that the silanization treatment of the lyophilized chitosan scaffolds could effectively promote the proliferation of Schwann cells in short time, which was promising candidate for *in vitro* cell attachment and growth in nerve regeneration application. But much further work should be perfomed to verify that in the future study.

4. Conclusion

In the present study, the porous chitosan scaffolds prepared by a freeze-drying method were silanized with APTE. Compared with single chitosan scaffolds, the APTE silanized scaffolds with high concentration showed a skin-like surface. The silanization treatment increased the porosity while reduced the swelling ratio of chitosan scaffolds, and the surface amino densities also increased with APTE concentration. The degradation behavior showed that the silanized chitosan scaffolds possessed improved degradation property in PBS and anti-acid dissolution properties. The results of *in vitro* Schwann cells culture suggested that the silanized scaffolds with 8% APTE could obviously promote the attachment and proliferation of Schwann cells, which may be promising for the application in peripheral nerve regeneration.

Acknowledgements

The authors gratefully acknowledge the financial support of the Natural Science Research Program of Jiangsu Education Department (No. 13KJB310014), Hi-Tech Research and Development Program of China (No. 2012AA020502), National Natural Science Foundation of China (No. 21242005, 81130080 and 81171457), Natural Science Foundation of Nantong City (No. BK2012089), Natural Science Foundation of Jiangsu Province of China (No. BK20130390) and the Natural Science Foundation of Nantong University (No. 10Z014).

References

Annabi, N., Nichol, J. W., Zhong, X., Ji, C., Koshy, S., Khademhosseini, A., et al. (2010). Controlling the porosity and microarchitecture of hydrogels for tissue engineering. *Tissue Engineering, Part B: Review*, *16*, 371–383.

Baggi, L., Boschi, M., Caleffi, A., Martignoni, M., & Venanzi, L. (1990). Silane coupling agents. *Attualita Dentale*, *6*, 18–21.

Busilacchi, A., Gigante, A., Mattioli-Belmonte, M., Manzotti, S., & Muzzarelli, R. A. (2013). Chitosan stabilizes platelet growth factors and modulates stem cell differentiation toward tissue regeneration. *Carbohydrate Polymers*, *98*, 665–676.

Byrne, E. M., Farrell, E., McMahon, L. A., Haugh, M. G., O'Brien, F. J., Campbell, V. A., et al. (2008). Gene expression by marrow stromal cells in a porous collagen-glycosaminoglycan scaffold is affected by pore size and mechanical stimulation. *Journal of Materials Science Materials in Medicine*, *19*, 3455–3463.

Chiono, V., Tonda-Turo, C., & Ciardelli, G. (2009). Chapter 9: Artificial scaffolds for peripheral nerve reconstruction. *International Review of Neurobiology*, *87*, 173–198.

Gan, S., Yang, P., & Yang, W. (2009). Photoactivation of alkyl C—H and silanization: A simple and general route to prepare high-density primary amines on inert polymer surfaces for protein immobilization. *Biomacromolecules*, *10*, 1238–1243.

Gu, Y., Ji, Y., Zhao, Y., Liu, Y., Ding, F., Gu, X., et al. (2012). The influence of substrate stiffness on the behavior and functions of Schwann cells in culture. *Biomaterials*, *33*, 6672–6681.

Halliwell, C. M., & Cass, A. E. (2001). A factorial analysis of silanization conditions for the immobilization of oligonucleotides on glass surfaces. *Analytical Chemistry*, *73*, 2476–2483.

Hennink, W. E., & van Nostrum, C. F. (2002). Novel crosslinking methods to design hydrogels. *Advanced Drug Delivery Reviews*, *54*, 13–36.

Howarter, J. A., & Youngblood, J. P. (2006). Optimization of silica silanization by 3-aminopropyltriethoxysilane. *Langmuir*, *22*, 11142–11147.

Hsu, S. H., Chan, S. H., Chiang, C. M., Chen, C. C. C., & Jiang, C. F. (2011). Peripheral nerve regeneration using a microporous polylactic acid asymmetric conduit in a rabbit long-gap sciatic nerve transection model. *Biomaterials*, *32*, 3764–3775.

Ichihara, S., Inada, Y., Nakada, A., Endo, K., Azuma, T., Nakai, R., et al. (2009). Development of new nerve guide tube for repair of long nerve defects. *Tissue Engineering Part C: Methods*, *15*, 387–402.

Kim, J. (2011). Formation, structure, and reactivity of amino-terminated organic films on silicon substrates. *Interfaces and Interphases in Analytical Chemistry*, *1062*, 141–165.

Kuo, Y. C., & Chang, Y. H. (2013). Differentiation of induced pluripotent stem cells toward neurons in hydrogel biomaterials. *Colloids and Surfaces B: Biointerfaces*, *102*, 405–411.

Kuo, Y. C., & Lin, C. C. (2013). Accelerated nerve regeneration using induced pluripotent stem cells in chitin–chitosan–gelatin scaffolds with inverted colloidal crystal geometry. *Colloids Surf B: Biointerfaces*, *103*, 595–600.

Lapin, N. A., & Chabal, Y. J. (2009). Infrared characterization of biotinylated silicon oxide surfaces, surface stability, and specific attachment of streptavidin. *Journal of Physical Chemistry B*, *113*, 8776–8783.

Li, G., Yang, P., Qin, W., Maitz, M. F., Zhou, S., & Huang, N. (2011). The effect of coimmobilizing heparin and fibronectin on titanium on hemocompatibility and endothelialization. *Biomaterials*, *32*, 4691–4703.

Matinlinna, J. P., & Vallittu, P. K. (2007). Silane based concepts on bonding resin composite to metals. *Journal of Contemporary Dental Practice*, *8*, 1–8.

Muzzarelli, R. A. A. (2009). Chitins and chitosans for the repair of wounded skin, nerve, cartilage and bone. *Carbohydrate Polymers*, *76*, 167–182.

Nie, X., Deng, M., Yang, M., Liu, L., Zhang, Y., & Wen, X. (2013). Axonal regeneration and remyelination evaluation of chitosan/gelatin-based nerve guide combined with transforming growth factor-beta1 and Schwann Cells. *Cell Biochemistry and Biophysics*.

Peng, L., Cheng, X. R., Wang, J. W., Xu, D. X., & Wang, G. (2006). Preparation and evaluation of porous chitosan/collagen scaffolds for periodontal tissue engineering. *Journal of Bioactive and Compatible Polymers*, *21*, 207–220.

Pettersson, J., McGrath, A., Kalbermatten, D. F., Novikova, L. N., Wiberg, M., Kingham, P. J., et al. (2011). Muscle recovery after repair of short and long peripheral nerve gaps using fibrin conduits. *Neuroscience Letters*, *500*, 41–46.

Qu, D., Lin, H., Zhang, N., Xue, J., & Zhang, C. (2013). In vitro evaluation on novel modified chitosan for targeted antitumor drug delivery. *Carbohydrate Polymers*, *92*, 545–554.

Runge, M. B., Dadsetan, M., Baltrusaitis, J., Knight, A. M., Ruesink, T., Lazcano, E. A., et al. (2010). The development of electrically conductive polycaprolactone

fumarate-polypyrrole composite materials for nerve regeneration. *Biomaterials*, *31*, 5916–5926.
Salon, M. C., Abdelmouleh, M., Boufi, S., Belgacem, M. N., & Gandini, A. (2005). Silane adsorption onto cellulose fibers: Hydrolysis and condensation reactions. *Journal of Colloid and Interface Science*, *289*, 249–261.
Wang, X., Hu, W., Cao, Y., Yao, J., Wu, J., & Gu, X. (2005). Dog sciatic nerve regeneration across a 30-mm defect bridged by a chitosan/PGA artificial nerve graft. *Brain*, *128*, 1897–1910.
Wlaszczuk, A., Pietrucha-Dutczak, M., Marcol, W., Jedrzejowska-Szypulka, H., & Lewin-Kowalik, J. (2011). The use of chitosan to facilitate nerve regeneration. *Wiadomosci Lekarskie*, *64*, 208–216.
Xiao, W., Hu, X. Y., Zeng, W., Huang, J. H., Zhang, Y. G., & Luo, Z. J. (2013). Rapid sciatic nerve regeneration of rats by a surface modified collagen–chitosan scaffold. *Injury*.
Xu, H., Yan, Y., & Li, S. (2011). PDLLA/chondroitin sulfate/chitosan/NGF conduits for peripheral nerve regeneration. *Biomaterials*, *32*, 4506–4516.
Yang, Y., Zhao, W., He, J., Zhao, Y., Ding, F., & Gu, X. (2011). Nerve conduits based on immobilization of nerve growth factor onto modified chitosan by using genipin as a crosslinking agent. *European Journal of Pharmaceutics and Biopharmaceutics*, *79*, 519–525.
Yannas, I. V., Lee, E., Orgill, D. P., Skrabut, E. M., & Murphy, G. F. (1989). Synthesis and characterization of a model extracellular matrix that induces partial regeneration of adult mammalian skin. *Proceedings of the National Academy of Sciences of the United States of America*, *86*, 933–937.
Yoshioka, T., Tsuru, K., Hayakawa, S., & Osaka, A. (2003). Preparation of alginic acid layers on stainless-steel substrates for biomedical applications. *Biomaterials*, *24*, 2889–2894.
Yuan, Y., Zhang, P., Yang, Y., Wang, X., & Gu, X. (2004). The interaction of Schwann cells with chitosan membranes and fibers in vitro. *Biomaterials*, *25*, 4273–4278.
Zhang, L., Dou, S., Li, Y., Yuan, Y., Ji, Y., Wang, Y., et al. (2013). Degradation and compatibility behaviors of poly(glycolic acid) grafted chitosan. *Materials Science and Engineering C: Materials for Biological Applications*, *33*, 2626–2631.
Zhu, Y., Gao, C., Liu, X., & Shen, J. (2002). Surface modification of polycaprolactone membrane via aminolysis and biomacromolecule immobilization for promoting cytocompatibility of human endothelial cells. *Biomacromolecules*, *3*, 1312–1319.